

## Article

# The Different Effect of Decellularized Myocardial Matrix Hydrogel and Decellularized Small Intestinal Submucosa Matrix Hydrogel on Cardiomyocytes and Ischemic Heart

Xifeng Yang <sup>1</sup>, Shihao Chen <sup>1</sup>, Jiaxin Chen <sup>2</sup>, Yunqi Liu <sup>3</sup>, Ying Bai <sup>2</sup>, Shengli Yin <sup>3,\*</sup> and Daping Quan <sup>2,\*</sup> 

<sup>1</sup> PCFM Laboratory, Guangdong HPPC Laboratory, School of Chemistry, Sun Yat-sen University, Guangzhou 510275, China; yangxf@mail2.sysu.edu.cn (X.Y.); chshihao@mail2.sysu.edu.cn (S.C.)

<sup>2</sup> Guangdong Functional Biomaterials Engineering Technology Research Center, School of Materials Science and Engineering, Sun Yat-sen University, Guangzhou 510275, China; chenjx383@mail2.sysu.edu.cn (J.C.); baiy28@mail.sysu.edu.cn (Y.B.)

<sup>3</sup> Department of Cardiac Surgery, The First Affiliated Hospital, Sun Yat-sen University, Guangzhou 510080, China; lyunq@mail.sysu.edu.cn

\* Correspondence: yinshl@mail.sysu.edu.cn (S.Y.); cesqdp@mail.sysu.edu.cn (D.Q.); Tel.: +86-2084114030 (D.Q.)

**Abstract:** Injectable decellularized matrix hydrogels derived from either myocardium or small intestinal submucosa (pDMYO-gel, pDSIS-gel) have been successfully used for myocardial injury repair. However, the relationship between tissue-specific biological functions and protein composition in these two materials is not clear yet. In this study, the protein composition, mechanical properties, and morphology of these two hydrogels and their effects on the behavior of neonatal rat cardiomyocytes (NRCMs) and human umbilical vein endothelial cells (HUVECs), are investigated. The results show that pDMYO-gel is more conducive to growth, adhesion, spreading, and maintenance of normal NRCM beating, due to its higher proportion of extracellular matrix (ECM) glycoproteins (49.55%) and some unique functional proteins such as annexin-6 (ANXA6), agrin (AGRN), cathepsin D (CTSD) and galectin-1 (LGALS1), whereas pDSIS-gel is more conducive to the proliferation of HUVECs. Animal study shows that pDMYO-gel has a better effect on improving cardiac function, inhibiting myocardial fibrosis and maintaining ventricular wall thickness in acute myocardial infarction models in vivo. Therefore, it is proposed that injectable pDMYO-gel hydrogel may be more suitable for functional recovery of myocardial injuries.

**Keywords:** decellularized matrix hydrogels; protein composition; cardiomyocytes; proteomic analysis; myocardial infarction



**Citation:** Yang, X.; Chen, S.; Chen, J.; Liu, Y.; Bai, Y.; Yin, S.; Quan, D. The Different Effect of Decellularized Myocardial Matrix Hydrogel and Decellularized Small Intestinal Submucosa Matrix Hydrogel on Cardiomyocytes and Ischemic Heart. *Appl. Sci.* **2021**, *11*, 7768. <https://doi.org/10.3390/app11177768>

Academic Editor: Giuseppina Andreotti

Received: 9 July 2021

Accepted: 20 August 2021

Published: 24 August 2021

**Publisher's Note:** MDPI stays neutral with regard to jurisdictional claims in published maps and institutional affiliations.



**Copyright:** © 2021 by the authors. Licensee MDPI, Basel, Switzerland. This article is an open access article distributed under the terms and conditions of the Creative Commons Attribution (CC BY) license (<https://creativecommons.org/licenses/by/4.0/>).

## 1. Introduction

Myocardial infarction is one of the most common coronary heart diseases. After myocardial infarction, inflammatory cells infiltrate the infarct area, and secrete matrix metalloproteinases and other active degradation substances that degrade the extracellular matrix, leading to replacement of the infarct area by scar fibrous tissues. The loss of extracellular matrix support in the infarct border induces necrosis or apoptosis of the cardiomyocytes, which further leads to continuous physiological changes, such as infarct area expansion, and ultimately causes final heart failure and death. Current treatments for myocardial infarction, including drug therapy and myocardial reperfusion, does not repair the myocardium. Biomaterials provide new options for the treatment of myocardial injuries after myocardial infarction. These materials mainly include synthetic [1–3], natural [4–8], and biological materials [9–11]. Biological tissue-derived decellularized matrices have excellent cell affinity due to their large content in bioactive substances, such as collagen, glycosaminoglycans (GAG), proteoglycans, various growth factors, and other bioactive components, all promoting specific cell growth, differentiation, endogenous tissue regeneration, and repair. Thus, in recent years, researchers in the field have put a special

focus on tissue-derived decellularized matrices [12]. Porcine decellularized small intestinal submucosa matrix (pDSIS), porcine decellularized myocardial matrix (pDMYO), and human decellularized amniotic membrane/human decellularized placenta (HDAM/HDP) matrices have been used to repair myocardial infarction [9–11,13]. Two of them, pDSIS myocardial patch (CorMatrix™) and pDMYO injectable hydrogel (Ventrigel™), have already been commercialized.

There are unique advantages in clinical application for injectable hydrogels since they can be directly injected into the injured site through minimally invasive surgery and form hydrogel in situ. Several studies demonstrated in different animal models that decellularized matrix hydrogels derived from diverse tissues can effectively repair myocardial injuries. Boyd et al. [9] prepared pDSIS hydrogels to repair porcine myocardial infarction and found that, compared with untreated animals, the cardiac functions of treated pigs, including ejection fraction and end systolic volume, were significantly improved. Francis et al. [10] used HDP hydrogel to repair acute myocardial infarction in rats. Compared with that of control animals injected with a saline solution, the scar tissue of myocardial infarction area in treated animals was significantly reduced, and the surviving tissue maintained normal electrophysiological activity. Singelyn et al. [11] prepared pDMYO hydrogels to repair myocardial infarction in rats. This hydrogel recruited endogenous cardiomyocytes and improved cardiac contractions.

Although decellularized matrix hydrogels from different tissues display some repairing effects in myocardial injury, whether and how exactly their material source affects their repair effectiveness remains unclear. It is likely there is a correlation based on previous research showing that extracellular matrix materials have tissue specificity. Decellularized matrix hydrogels derived from peripheral nerves (DNM-G) can promote myelination of axons [14] but are not conducive to synapse formation. Meanwhile, hydrogels derived from spinal cord decellularized matrix facilitate the survival, proliferation, and migration of neural stem/progenitor cells (NSPCs), and promote NSPCs neuronal differentiation [15]; nucleus pulposus decellularized matrix hydrogels derived from intervertebral discs are beneficial to the differentiation of mesenchymal stem cells (MSCs) into nucleus pulposus-like cells; and decellularized matrix hydrogels from annulus fibrosus facilitate the differentiation of MSCs into annulus fibrosus-like cells [16]. Ungerleider et al. [17] also found that skeletal muscle and human umbilical cord-derived decellularized hydrogels can repair peripheral arterial disease in a rat hind limb ischemia model, and the former reconstructed muscle tissue was closer to natural healthy skeletal muscle.

Several studies showed that protein composition found in decellularized matrices derived from specific tissue has specific biological function on the target tissue. As previously shown that DNM-G preserved critical biological factors unique of peripheral nerve which facilitated myelination. Proteins found in DNM-G only, such as collagen IV  $\alpha$ 1, collagen IV  $\alpha$ 2, and collagen V  $\alpha$ 2, show a positive correlation with regulation for myelination [14]. There are 22 and 16 specific ECM matrisome proteins for the decellularized spinal cord matrix (DSCM) and decellularized peripheral nerve matrix, respectively. The DSCM specific glycoprotein and secreted factor, tenascin family, and fibroblast growth factor 2, are proved to be able to promote the NSPCs proliferation [15]. For regeneration of complex tissues, a study from Cunniffe et al. [18] showed that specific proteins were found in scaffolds derived from Growth plate ECM, such as chondroitin sulfate proteoglycan 4 and angiopoietin like 2, which are believed to play a role in angiogenesis; and C-Type Lectin Domain Containing 11A, Matrix Metalloproteinase 13 and S100 Calcium-Binding Protein A10, which can promote osteogenesis. In contrast, specific proteins were found in scaffolds derived from articular cartilage ECM, such as Gremlin 1, Frizzled Related Protein, and Transforming Growth Factor Beta 1, which can inhibit hypertrophy and promote chondrogenesis.

Therefore, the comparison of pDSIS-gel to pDMYO-gels in order to determine tissue-specific advantages for myocardial injury repair in animals, the relationship between the protein composition in pDMYO and potential tissue-specific biological functions needs to

be defined. To this end, this study investigated the micromorphology, mechanical strength, composition, effect on cardiac-related cell behavior *in vitro*, and cardiac function in rat acute myocardial infarction models *in vivo* of these two gels. The ultimate aim was to correlate the differential effects exerted by these two gels on cell.

## 2. Materials and Methods

### 2.1. Materials and Reagents

Male landrace pigs (8-month-old,  $\approx 48$  kg) were supplied by The Original Pig Farm, South China Agricultural University, China. Sprague-Dawley neonatal rats and adult male rats were supplied by the Laboratory Animal Center of Sun Yat-sen University, China. Collagen I (#354249) was purchased from Corning Incorporated, Corning, NY, USA. DNA extraction kit, DNA detection kit, PageRuler pre-staining protein marker, colorimetric peptide assay kit, silver plating staining kit, liquid chromatography column, and live/dead cell staining solution were purchased from Thermo Fisher Scientific, Inc., Waltham, MA, USA. A commercially available kit containing a 1,9-dimethylmethylene blue (DMMB) dye-binding assay was purchased from Genmed Scientifics Inc., Arlington, MA, USA. The hydroxyproline test kit was purchased from Nanjing Jiancheng Bioengineering Institute, Nanjing, China. Cell Counting Kit-8 was purchased from Dojindo, Kumamoto, Japan. Trypsin was purchased from Promega, Fitchburg, WI, USA. Pepsin, collagenase, DMEM/F12 basic medium, Complete medium/DMEM/F12, fetal bovine serum, horse serum, and penicillin, were purchased from GIBCO, Grand Island, NY, USA. Anti-cTn1 (#SAB4500539), -Cx43 (#SAB4301326) antibodies, and DAPI were purchased from Abcam, Cambridge, UK. Human umbilical vein endothelial cells (HUVECs) were purchased from ScienCell, Carlsbad, CA, USA. Triton X-100, sodium deoxycholate, tetramethylethylenediamine (TEMED), trimethylol aminomethane (Tris), urea (UA), iodoacetamide (IAA), dithiothreitol (DTT), formic acid (FA), triethylammonium bicarbonate (TEAB), trifluoroacetic acid, 5-bromodeoxyuridine (BrdU), and paraformaldehyde, were purchased from Sigma Aldrich, St. Louis, MO, USA. Dichloromethane and other reagents were purchased from Guangzhou Chemical Reagent Factory, Guangzhou, China.

### 2.2. Preparation of Decellularized Matrix and Hydrogel

The inner and outer membranes, fat, nerves, and blood vessels were dissected from the porcine heart and discarded, and the porcine myocardial tissues were washed and cut into pieces about 2-mm thick. The porcine small intestine was first washed with sterilized water, and then the submucosa was separated from the small intestine, scraped, and cut into pieces. The pieces were washed with sterilized water, soaked in 3% Triton X-100 for 24 h, and then soaked in 4% sodium deoxycholate on a shaker for 24 h. The small intestinal submucosa was degreased in dichloromethane/ethanol ( $v/v = 2/1$ ) for 24 h. Finally, the decellularized matrix was soaked 4–6 times for 12 h in sterilized water on a shaker, and finally lyophilized.

The lyophilized decellularized matrix was milled into powders using Mini-Mill (Thomas Wiley), and sieved with an 80-mesh sieve. A definite mass ( $M$ ) of powder was digested with pepsin ( $m$ ) ( $M:m = 10:1$ ). A 1 mg/mL pepsin solution was prepared in 0.01 M HCl. The digestion was stirred at room temperature for 24 h and stored at 4 °C. The pH of the digestion was adjusted to 8.0–8.5 with 1 M NaOH, and then 1 M HCl was used to adjust the pH value to 7. A 10 $\times$  phosphate-buffered saline (PBS) solution was used for isotonic equilibrium to obtain a pre-hydrogel at 4 °C. A hydrogel was obtained by increasing temperature of pre-hydrogel from 4 °C to 37 °C. The two different hydrogels prepared from the small intestine and heart were abbreviated pDSIS-gel and pDMYO-gel, respectively. Collagen type I hydrogel was prepared according to the instruction manual provided by Corning Incorporated and abbreviated COL1-gel. The above procedures were carried out under aseptic conditions. The concentration of each hydrogel was 5 mg/mL.

### 2.3. Characterization of Decellularized Matrices and Hydrogels

Freshly isolated tissues and decellularized matrices were fixed in 4% paraformaldehyde, washed three times with distilled water, embedded, frozen, sectioned at low temperature, and stained with hematoxylin and eosin (H&E). The stained sections were photographed with a Nikon eclipse E100 microscope.

The DNA from freshly isolated tissues and decellularized matrices was extracted using a DNA extraction kit (Thermo Fisher Scientific, USA), and analyzed with Quant-iT™ PicoGreen™ dsDNA Assay Kit (Thermo Fisher Scientific, USA) according to the instruction manual provided by the manufacturer, using 485 nm as the excitation wavelength and 528 nm as the emission wavelength on a Synergy HTX microplate reader (Biotek, Santa Barbara, CA, USA), with triplicates for each group.

Total glycosaminoglycan (GAG) content was isolated from freshly isolated tissues and decellularized matrices by high salt extraction, and quantified with a kit (Genmed Scientifics Inc., USA) based on a dimethylmethylene blue colorimetric assay, according to the manufacturer's instructions.

Collagen content was determined indirectly by measuring hydroxyproline concentration, based on the fact that hydroxyproline represents 13.4% of the total amino acids contained in collagen. Freshly isolated tissues and decellularized matrix samples were hydrolyzed by alkali, hydroxyproline oxide, and dimethylaminobenzaldehyde, to produce a purplish red compound quantified by colorimetry.

The pepsin-digested porcine decellularized myocardial and intestinal submucosa matrices and the collagen solutions were analyzed and compared by SDS-PAGE, in 12% polyacrylamide separation gel and 5% polyacrylamide concentration gel. The electrophoresis was performed in a XCell SureLock Mini-Cell electrophoresis system (Thermo Fisher Scientific) and the proteins were detected by silver staining.

A scanning electron microscope (SEM, HITACHI S-4800, Japan) was used to analyze the hydrogel scaffolds. pDMYO-gel, pDSIS-gel, and COL1-gel at a concentration of 5 mg/mL were fixed in 2.5 wt% glutaraldehyde solution for 6 h. The samples were washed three times with deionized water for 30 min. Then, they were dehydrated successively in 30%, 50%, 75%, and 100% ethanol solutions for 30 min at each step. The samples were soaked in deionized water for 6 h, with the deionized water being changed every 2 h. The final hydrogel scaffolds were lyophilized. The samples were coated by platinum and observed by SEM. The SEM images were analyzed in the software ImageJ (version No. 1.53c). Three samples per experimental group were selected, and two SEM images/sample were analyzed. Ten fibers were randomly selected from each SEM image for diameter measurement and statistics.

The elastic storage modulus of the hydrogel scaffolds was tested in a Rotational Rheometer (Haake MARS, Thermo Fisher). The concentration of each tested sample was 5 mg/mL. The operation steps were as follows: 0.2 mL of hydrogel solution was placed on the parallel sample stand. Analysis was performed in flow mode and in conjunction with parallel steel plate geometry (20 mm diameter) with a gap of 0.5 mm. The temperature of the sample table was set at 4 °C. The test parameters were set at 1% strain and 1 Hz frequency. The temperature of the sample table rapidly raised from 4 °C to 37 °C (the heating rate was 200 °C per min) and maintained at 37 °C for 6 min. The elastic storage modulus (g) of each group was recorded.

### 2.4. Isolation of Neonatal Rat Cardiomyocytes (NRCMs)

Neonatal (1–3-day old) Sprague Dawley rats were anesthetized with ether, and their hearts were harvested. The hearts were washed in sterile phosphate buffer saline (PBS) containing 0.9 mM CaCl<sub>2</sub> and 0.5 mM MgCl<sub>2</sub> to induce cardiac contraction, and the corpuscles were removed. The hearts were then transferred to PBS buffer without CaCl<sub>2</sub> and MgCl<sub>2</sub>, and the ventricles were separated from the atrium and cut into 1-mm<sup>3</sup> pieces with thin scissors. The ventricular tissues were incubated in PBS containing 0.25% of collagenase at 37 °C for 30 min for digestion. After repeating the digestion procedure

twice, the cell suspension was transferred to cell culture medium supplemented with 10% fetal bovine serum and 100 U/mL penicillin, and the cells were filtered through a 40  $\mu\text{m}$ -diameter nylon mesh. The samples were centrifuged at room temperature at  $180\times g$  for 5 min. The cells were resuspended in cell culture medium and incubated for 60 min. The non-adherent cells were centrifuged, resuspended in cell culture medium containing BrdU, and transferred to a new culture dish.

#### 2.5. Culture of NRCMs and Human Umbilical Vein Endothelial Cells (HUVECs) on Hydrogels

Seven microliters of the pre-hydrogels from Section 2.2 were added to the wells of a 48-well plate at 4 °C, respectively. Then the hydrogels were formed by increasing temperature of the pre-hydrogels from 4 °C to 37 °C. The extracted NRCMs were seeded on the formed hydrogels at a concentration of  $8 \times 10^4$  cells per well, and cultured in complete medium/DMEM/F12. After passage, HUVECs were seeded on the formed hydrogels at  $2 \times 10^4$  cells per well, respectively, and cultured in complete medium/DMEM/F12.

#### 2.6. Monitoring of Myocardial Cell Survival on Gel Materials by Live/Dead Staining

After cultured for three days, NRCMs and HUVECs were stained with live/dead dye and photographed. The culture medium was removed by aspiration and the cells were washed in PBS 1–2 times. The following steps were performed in dark condition. One milliliter of live/dead dye solution was prepared in PBS by mixing 2  $\mu\text{M}$  live green and 4  $\mu\text{M}$  dead red dyes, and 100  $\mu\text{L}$  of this solution was added per culture well. The cells were completely immersed and incubated at room temperature for 10 min. Finally, the dye was removed by aspiration, the cells were washed three times in PBS solution, and the samples were observed and photographed under a Leica SP8 confocal microscope (Wetzlar, Germany).

#### 2.7. Detection of NRCMs and HUVECs Viability on Gel Materials

After one, three, and seven days in culture, the viability of the NRCMs was assessed with the Cell Counting Kit-8 assay (CCK8) colorimetric method. The HUVECs were assessed with the same method after one, two, and three days of culture. Briefly, the CCK-8 solution (10  $\mu\text{L}$ ) was added to each culture well, the plates were cultured at 37 °C for 4 h. The absorbance was read in a microplate reader (Thermo Scientific, Waltham, MA, USA) at 450 nm.

#### 2.8. Immunofluorescence Staining

After three days in culture, the NRCMs were characterized by immunofluorescence staining with anti-cTnI and anti-Cx43 antibodies. The protocol was as follows: the culture medium was removed by aspiration, and the cardiomyocyte cultures were washed 1–2 times with PBS. The cells were fixed in 4% paraformaldehyde for 30 min and washed several times with PBS for 5 min. They were permeabilized with 0.3% Triton X-100 for 30 min at room temperature, and after removal of the permeabilization solution, they were blocked with 10% horse serum for 30 min at 37 °C. Then the primary antibody was added. According to the recommended the anti-cTnI antibody was diluted at 1:200, the anti-Cx43 antibody was diluted at 1:2000, and incubated with the cells overnight at 4 °C. The first antibody was removed by aspiration and the cells were washed three times with PBS for 5 min. The second fluorescent antibody was added according at the dilution indicated by the manufacturer and incubated at room temperature for 2 h in the dark. The samples were maintained in the dark. After removing the fluorescent secondary antibody by aspiration, the cells were washed three times with PBS for 3 min. DAPI diluted at 1:200 was added to stain the nucleus. The cells were incubated in dark for 15 min at room temperature. Finally, the cells were washed three times with PBS for 5 min. The staining images were observed under a Leica SP8 confocal microscope (Wetzlar, Germany).

### 2.9. Measurement of Cardiomyocyte Beating Frequency

Cardiomyocyte function was assessed by quantifying the beating frequency of the cardiomyocytes maintained in hydrogel culture for eight days. The beating frequency of NRCMs cultured on different materials for one to eight days was monitored, counted under a microscope, and recorded manually twice daily (interval > 3 h, observation window < 15 min).

### 2.10. Liquid Chromatography-Tandem Mass Spectrometry (LC-MS) Analysis

#### 2.10.1. Protein Digestion and Peptide Extraction

Protein digestion and peptide extraction from the decellularized matrices were conducted as reported previously. [15] Briefly, Ultrafiltration-assisted sample preparation was used for protein digestion. A sample of 300  $\mu$ L UA solution (8 M urea dissolved in 0.1 M Tris HCl, pH 8.5) was used for diluting samples. A 10-kDa filter was used for centrifuging. A 200- $\mu$ L UA solution with 50 mM DTT was used for reduction of samples. A 200- $\mu$ L UA solution with 100 mM IAA was used for sample alkylation. After sample alkylation, a 200- $\mu$ L UA solution was used for sample rinsing twice and a 200- $\mu$ L TEAB solution (50 mM) was for rinsing for five times. The sample was centrifugated at  $12,000\times g$  for 12 min at room temperature after each rinsing. A 100- $\mu$ L TEAB solution containing 2  $\mu$ g Trypsin Gold (Promega, USA) was used for digestion at 37 °C for 18 h. The resulted peptide was collected centrifugation at  $12,000\times g$  for 15 min at least twice. A 100- $\mu$ L TEAB solution was added after each centrifugation. The final peptide concentration was tested by a pierce quantitative colorimetric peptide assay (Thermo Fisher Scientific). Lyophilization and desalination were performed on the peptide mixture. Finally, the peptide samples were lyophilized again and stored at  $-20\text{ }^{\circ}\text{C}$  until LC-MS analysis.

#### 2.10.2. LC-MS Analysis

LC-MS analysis was conducted as reported previously [15]. Briefly, a nanoflow high-performance liquid chromatograph (HPLC) system (Easy nLC1200 system, Thermo Fisher Scientific, USA) coupled to an Orbitrap Q Exactive HF-X mass spectrometer (Thermo Fisher Scientific, USA) with a nanoelectrospray ion source (Thermo Fisher, USA) was used. The sample dissolved in buffer A (0.1% formic acid [FA]) was injected into a 2-cm trap column (75- $\mu$ m inner diameter, Acclaim PepMap 100C18, 3  $\mu$ m, Thermo Scientific) and separated on a 75- $\mu$ m-inner-diameter column with a length of 25 cm (Acclaim PepMap 100C18, 2  $\mu$ m; Thermo Scientific) over a 120-min gradient (buffer A, 0.1% FA in water; buffer B, 0.1% FA in 80% Acetonitrile [ACN]) at a flow rate of 300 nL/min (0–3 min, 3–8% B; 3–99 min, 8–28% B; 99–113 min, 28–33% B; 113–116 min, 33–98% B; and 116–120 min, 98% B). The Q Exactive HF mass spectrometer was operated in positive ion mode at ion transfer tube temperature 320 °C, and the positive ion spray voltage was 3.7 kV. MS scans were acquired at resolution of 60,000, and the maximum injection time was 50 ms. High-energy collisional dissociation fragmentation was carried out at 28% normalized collision energy. MS2 AGC target was set to  $1\times 10^5$ , the maximum injection time was set to 30 ms, and the dynamic exclusion was set to 60 s.

The MS data were searched against the Sus scrofa (pig) UniProt database (taxon identifier 9823, version 2018061348865) using Proteome Discoverer (software version 2.3, Thermo Scientific). The Precursor\_Quan\_LFQ\_Sequest™ HT search engine was used to search the data. The search parameters were set as follows: trypsin was selected as proteolytic enzyme, and two missed cleavage sites were allowed; cysteine carbamylation was used as immobilization modification; oxidation of M and acetylation of N-terminal were used as modification variables; search quality tolerance was set as 10 ppm; false discovery rates of peptide-spectrum matching (PSMs) and protein were set as less than 1%.

### 2.11. Rat acute Myocardial Infarction Model and Injection of Decellularized Matrix Hydrogels

Adult male SD rats (450–650 g) were provided by the Laboratory Animal Center of Sun Yat-Sen University. All animals were housed in SFP animal facility. Food and water were available ad libitum.

The rats were randomly divided into four groups: Shame group, PBS group, pDSIS-gel and pDMYO-gel group ( $n = 8$  for 4 weeks each group).

The rats were anaesthetized using 10 wt% chloral hydrate solution (0.33 mL/100 g, i.p.). After anesthesia, the chest and neck were shaved and the skin was cleaned and disinfected. The anaesthetized rats were placed on a heatable operating table in supine position. Intubation was performed with an 18 G intravenous catheter, and the rats were ventilated with a volume-controlled small animal ventilator at 3 mL/100 g tidal volume at 60 breaths per minute.

The rat heart was surgically exposed with a left thoracotomy. After the pericardium was separated, the left anterior descending coronary artery was ligated with a 5–0 silk suture to induce ischemia in the distal regions of the left ventricular myocardium. The infarct site turned white rapidly, indicating successful ligation. PBS and pre-hydrogels were aspirated with 1 mL microinjector for 60  $\mu$ L. The experimental materials were injected at 3–4 sites on the border of myocardial infarction area in rats. After confirming that the material was successful injected and no malignant arrhythmia was found in the rats, the thoracic cavity was sutured layer by layer, and the ventilating was maintained continuously. During the whole process, the rats were placed on a heating pad to support the body temperature of the rats and promote the recovery of the rats. After the rats recovered, the intravenous catheter was removed. Finally, the rats were transferred to the animal cages for further breeding.

### 2.12. Echocardiography

Four weeks after surgery, the rats were anesthetized, and then fixed on the rat plate, coated with a small amount of couplant. Echocardiography was performed with small animal ultrasound equipment (Vevo 2100 Imaging System, vevo2100, Canada). Five cardiac cycles were recorded, as well as left ventricular ejection fraction (LVEF) and left ventricular fractional shortening (LVFS) with which reflecting cardiac function were measured.

### 2.13. Histology

The rats were sacrificed at four weeks after surgery for histological evaluation, and the whole heart was extracted. The isolated heart was cleaned with PBS and fixed with 4% paraformaldehyde and stored at 4 °C.

The specimens were embedded in paraffin, and were serially sectioned at a thickness of 3  $\mu$ m. After dewaxing, the slides were stained with H&E and Masson trichrome by Wuhan Servicebio Technology Co., Ltd. (Wuhan, China) and observed and photographed under Nikon eclipse E100. The obtained scanning section images were browsed by caseviewer software and analyzed by ImageJ image analysis software (version No. 1.53c).

### 2.14. Statistical Analysis

All statistical analyses were performed using GraphPad Prism 6.02 (GraphPad Software Inc., San Diego, CA, USA). Data are shown as mean  $\pm$  standard deviation. Data were analyzed using one-way analysis of variance (ANOVA) followed by Tukey's post hoc test. The values were considered significantly different at  $p < 0.05$ .

## 3. Results and Discussion

### 3.1. Preparation and Properties of the pDMYO- and pDSIS-Gels

The decellularization of porcine myocardial and small intestinal submucosa tissues were performed according to previously reported methods [11,19] (Figure 1A). After decellularization, there was no cell residue visible in either two materials stained with H&E (Figure 1B). The DNA content was  $56.39 \pm 1.0404$  ng per mg in pDMYO, and

$5.90 \pm 1.5151$  ng per mg in pDSIS, which is close to or lower than the minimum content (50 ng per mg) reported in a review [20]. These parameters met the basic biological safety criteria required for decellularized matrix materials prepared from biological tissues.

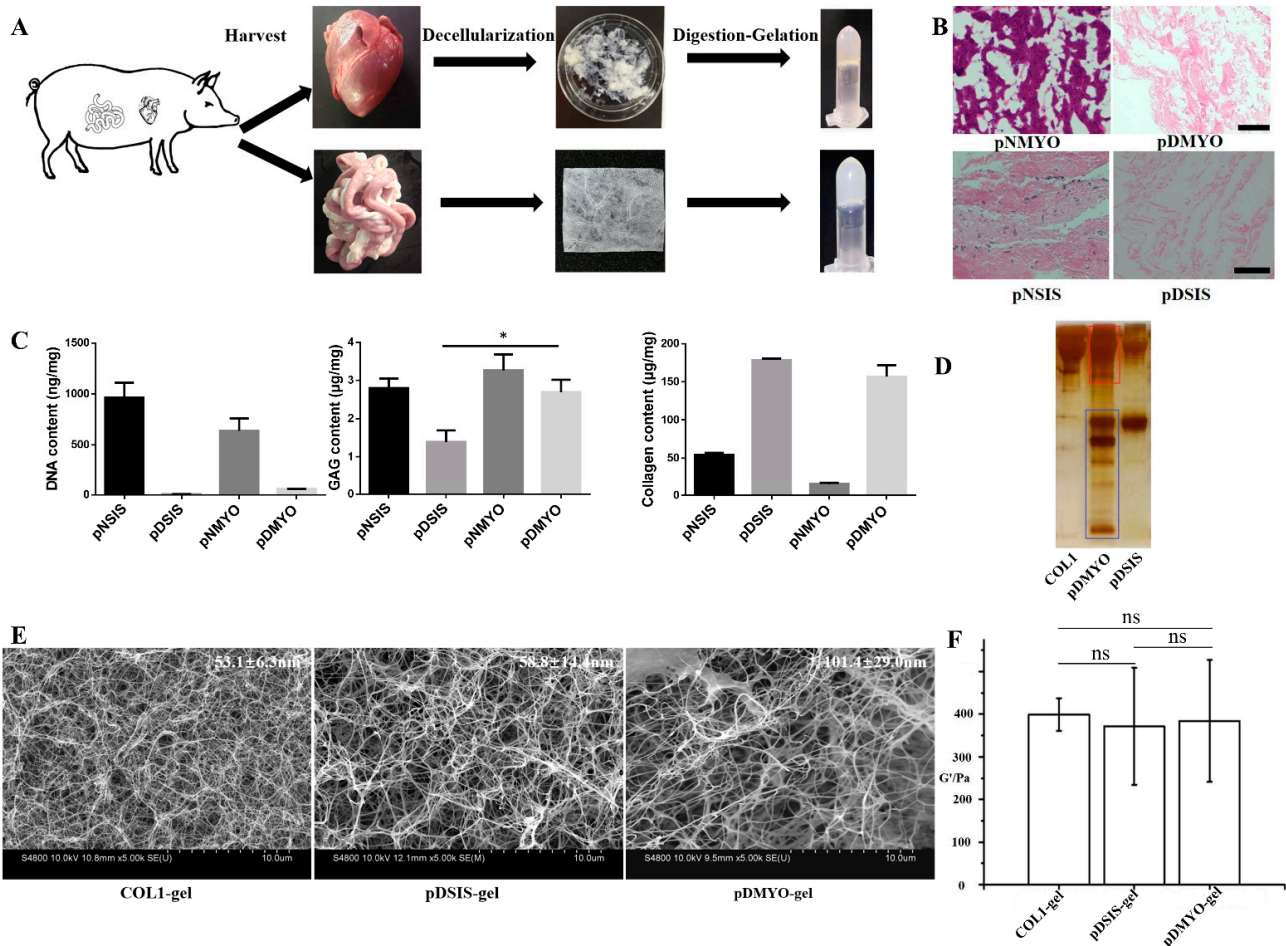


**Figure 1.** Preparation and properties of pDMYO-, pDSIS-, and COL1-gels. (A) Preparation of pDMYO- and pDSIS-gels; (B) H&E staining of porcine non-decellularized myocardial matrix (pNMYO) and porcine decellularized myocardial matrix (pDMYO), scale bar = 100  $\mu\text{m}$ ; H&E staining of porcine non-decellularized small intestinal submucosa matrix (pNSIS) and porcine decellularized small intestinal submucosa matrix (pDSIS), scale bar = 50  $\mu\text{m}$ ; (C) The contents of DNA, GAG and collagen in non-decellularized and decellularized materials; (D) Analysis of protein content in the three gels by SDS-PAGE. (E) Comparison of the three gels by scanning electron microscopy; (F) Comparison of the elastic modulus of the three gels. \* denotes statistical difference within the same group with  $p < 0.05$ , respectively ( $n = 3$ ).

GAG content was significantly higher in pDMYO ( $2.69 \pm 0.33$   $\mu\text{g}$  per mg) than in pDSIS ( $1.39 \pm 0.30$   $\mu\text{g}$  per mg), while collagen content was slightly lower in pDMYO ( $156.98 \pm 15.08$   $\mu\text{g}$  per mg) than in pDSIS ( $178.54 \pm 2.07$   $\mu\text{g}/\text{mg}$ ), which indicates that there was more GAG in pDMYO than in pDSIS (Figure 1C). As for the reason why the amount of GAG per mg of matrix decreases in decellularized material compared with non-decellularized material, yet the amount of collagen per mg increases. Firstly, the water content of fresh raw materials is higher than that of decellularized material. Therefore, the relative content of collagen in decellularized matrix material is increased compared with that in fresh raw materials. As for the content of glycosaminoglycan after acellularization, it is lower than that of fresh materials. The possible reason is that the decellularization method used in our study has a lower impact on collagen and a greater impact on GAG glycosaminoglycan. For example, Triton-X100 is a representative non-ionic detergent, which can effectively separate cell membrane-membrane connection and membrane-protein connection, while has little damage to protein-protein connection. Analysis by electrophoresis

showed that pDMYO contained more low molecular weight proteins than pDSIS, which indicated a higher complexity of the pDMYO components (Figure 1D). Compared with other hydrogels such as chitosan hydrogel [6], alginate hydrogel [7], hyaluronic acid hydrogel [8], the best of advantages is that there are more biological components in pDMYO-gel, including collagen, GAG and other low molecular weight proteins. This means that pDMYO-gel can be used to repair myocardial infarction alone or with other bioactive substances or cells, while other hydrogels usually are used as carriers only for carrying cells or other bioactive substances to repair myocardial infarction.

The analysis by SEM showed that our method of decellularized matrix preparation by digestion and jellification of two different tissues could successfully generate hydrogels with suitable nanofiber structures (Figure 1E). Fiber diameter in pDMYO-gel, with loose structure, was about 101.4 nm, while fiber diameter in pDSIS-gel was 58.8 nm, which was close to that found in collagen hydrogels (about 53.1 nm). These diameters were consistent with those previously reported for similar materials [21]. However, the rheological properties of the three hydrogels were not significantly different and had similar elastic modulus (Figure 1F).

### 3.2. Cell Compatibility and Ability to Support Cell Viability of pDMYO- and pDSIS-Gels

Neonatal rat cardiomyocytes (NRCMs) and human umbilical vein endothelial cells (HUVECs) were seeded and cultured on three different hydrogels. COL1-gel was taken as reference to investigate cell compatibility and viability on pDMYO- and pDSIS-gel. The three-day survival rate of the NRCMs was greater than 85% on the three hydrogels, and no significant difference was observed (Figure 2A,B). For the HUVECs, the three-day survival rate was greater than 98% for on all three gels, exceeding that of the NRCMs (Figure 2C,D).

NRCMs viability and cytotoxicity on the three hydrogels was tested using a CCK-8 assay. At one, three, and seven days, NRCMs survival was significantly higher on pDMYO-gel than on pDSIS- or COL1-gels (Figure 2E). In contrast, HUVECs viability was maintained for three days on the three hydrogels, and was the highest on pDSIS-gel (Figure 2F), which indicates pDSIS-gel can promote the proliferation of HUVECs better than other hydrogels.

### 3.3. Effects of pDMYO- and pDSIS-Gels on Cardiomyocyte Morphology and Function

Figure 3 shows images and corresponding beating rates of cardiomyocytes cultured for seven days on different hydrogels. The video capture (Figure 3A, Supplemental movies S1–S3) showed that cardiomyocytes cultured on pDMYO-gel were significantly stronger pulsatile and formed more intercellular connections compared to those cultured on other gels. The statistical analysis confirmed that the beating rate of NRCMs cultured on pDMYO-gel was highest at all times, during six days. The beating rates of the NRCMs cultured on the three different gels, in decreasing order, were pDMYO-gel pDSIS-gel COL1-gel (Figure 3B).

Cardiac troponin 1 (cTn1) is a regulatory protein of myocardial contraction only expressed in mature myocardium. Connexin 43 (Cx43) is the main protein component of the gap junctions in cardiomyocytes, and plays an important role in maintaining the connection, communication, signal transduction, and rhythmic contraction of the cardiomyocytes. Immunofluorescence staining images (Figure 3C,D) showed that the level of cTn1 and Cx43 expression in NRCMs cultured on pDMYO-gel was higher than that of the NRCMs cultured on pDSIS- or COL1-gels. This result was especially striking for the level of Cx43 expression, and was consistent with the results presented in Figure 3B. Thus, although pDSIS-gel can maintain the viability of cardiomyocytes and promote their maturation, it is inferior to pDMYO-gel in maintaining signal transduction and rhythmic contraction of the cardiomyocytes.

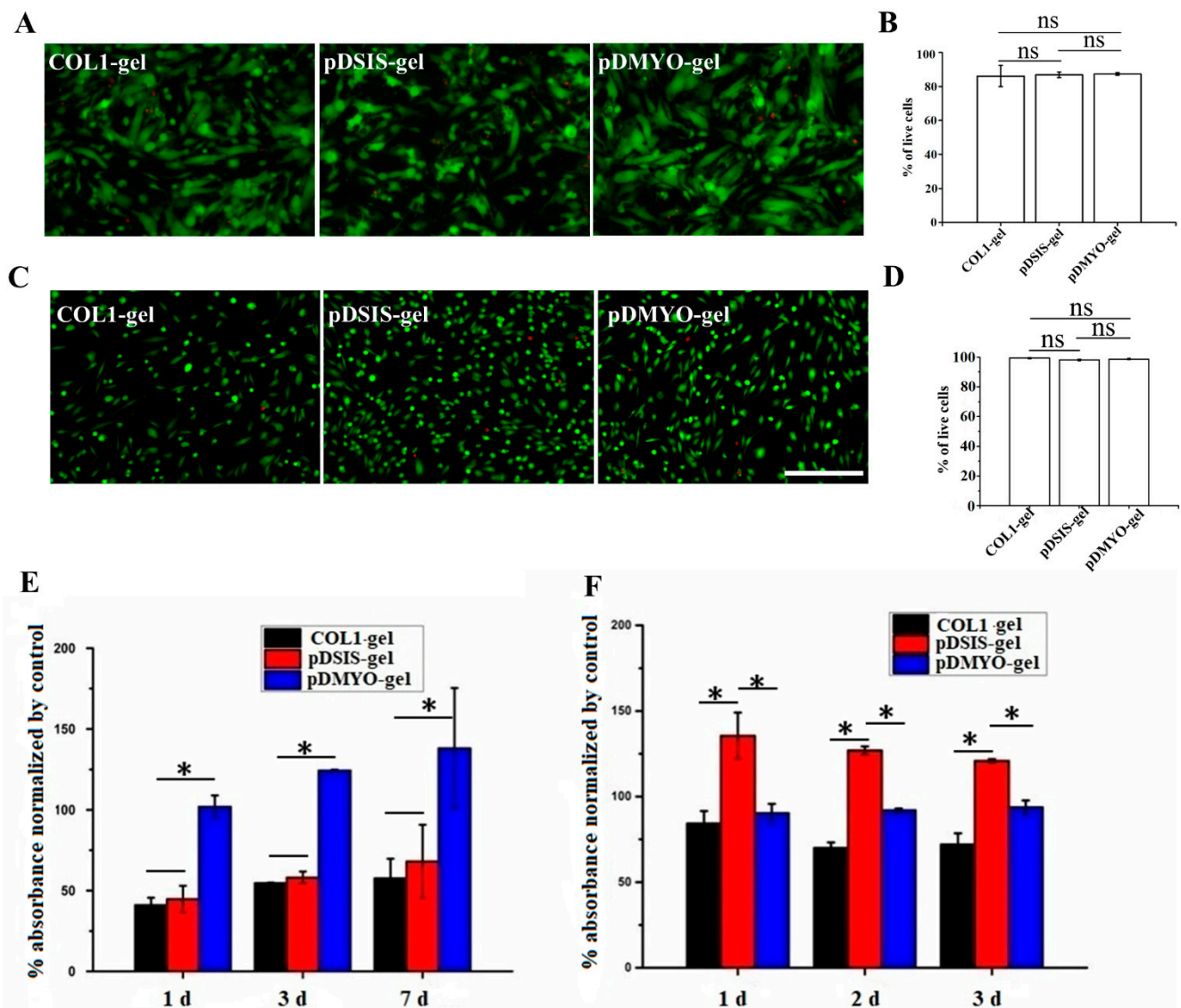


**Figure 2.** Assessment of the biocompatibility and capacity to sustain cell viability of the porcine decellularized matrix gels and collagen gels on myocardial-related cells. (A) Live/Dead staining of cardiomyocytes cultured on three different hydrogels after three days; scale bar = 500  $\mu$ m; (B) Survival rate of cardiomyocytes cultured on three different hydrogels; (C) Live/Dead staining of human umbilical vein endothelial cells cultures on three different hydrogels; scale bar = 500  $\mu$ m; (D) Survival rate of human umbilical vein endothelial cells on three different hydrogels; (E) Effect of three different hydrogels on cardiomyocytes viability; (F) Effect of three different hydrogels on human umbilical vein endothelial cell viability. \* denotes statistical difference within the same group with  $p < 0.05$ , respectively ( $n > 3$ ).

### 3.4. Proteomic Analysis of pDMYO and pDSIS

Proteomic analysis showed that pDMYO and pDSIS contained 944 and 161 different proteins, respectively, of which 154 were shared between the two matrices (Figure 4A,B). According to the protein categories, including ECM glycoproteins, ECM accessory proteins, ECM regulatory factors, proteoglycans, and secretory factors, all the protein contents of pDMYO were higher than those of pDSIS (Figure 4B). Figure 4C,D show the types of matrix histones and proportion of different proteins in pDMYO and pDSIS. The core matrisome proteins of pDMYO were dominantly ECM glycoproteins (49.6%), followed by collagen proteins (25.4%), whereas pDSIS was mainly composed of collagen proteins (72.1%), followed by ECM glycoproteins (15.2%) (Figure 4C,D). Furthermore, the secretory factors (1.37%) and ECM affiliated proteins (1.77%) were higher in pDMYO.

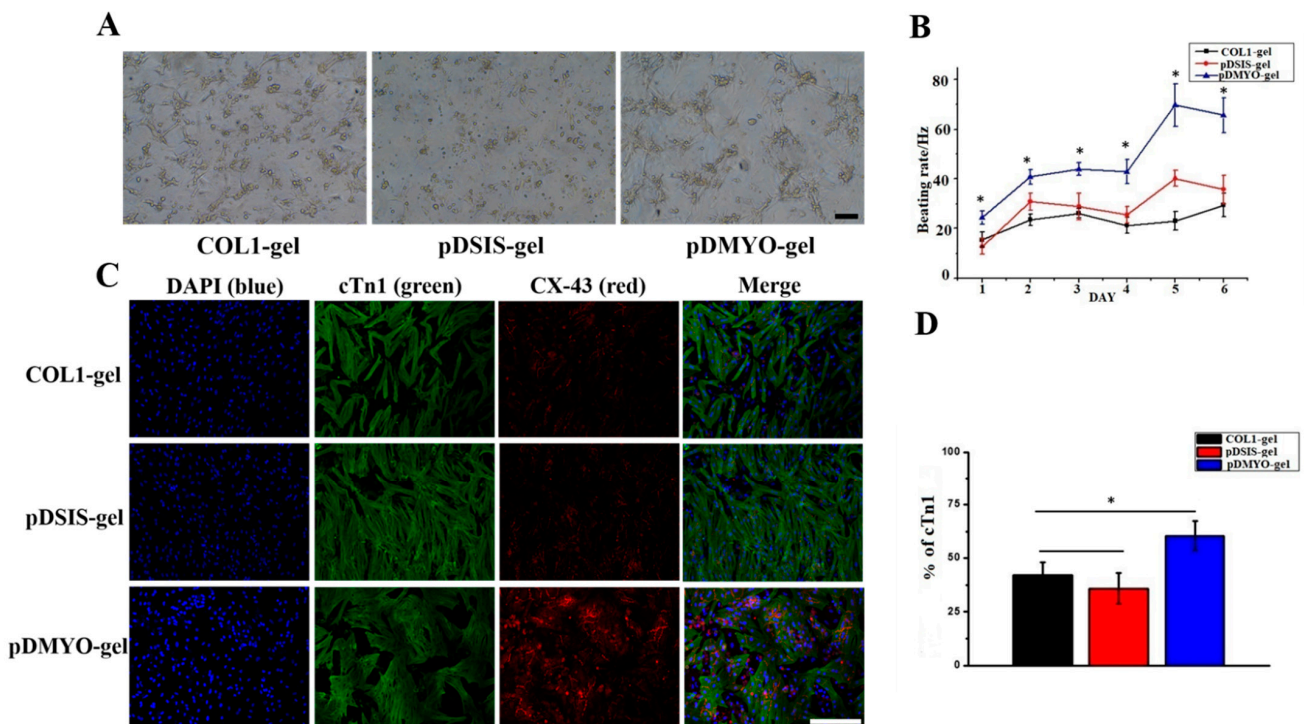


**Figure 3.** Effects of decellularized matrix and collagen hydrogel on cardiomyocytes morphology and function. (A) Video capture of beating cardiomyocytes after seven days in culture on different hydrogels; scale bar = 100 μm; (B) Effect of decellularized matrix and collagen hydrogels on cardiomyocyte beating rate; (C) Immunofluorescence staining of cardiomyocytes for cTnI (green) and Cx43 (red), scale bar = 500 μm; (D) Statistical analysis of cTnI expression. \* denotes statistical difference within the same group with  $p < 0.05$ , respectively ( $n > 3$ ).

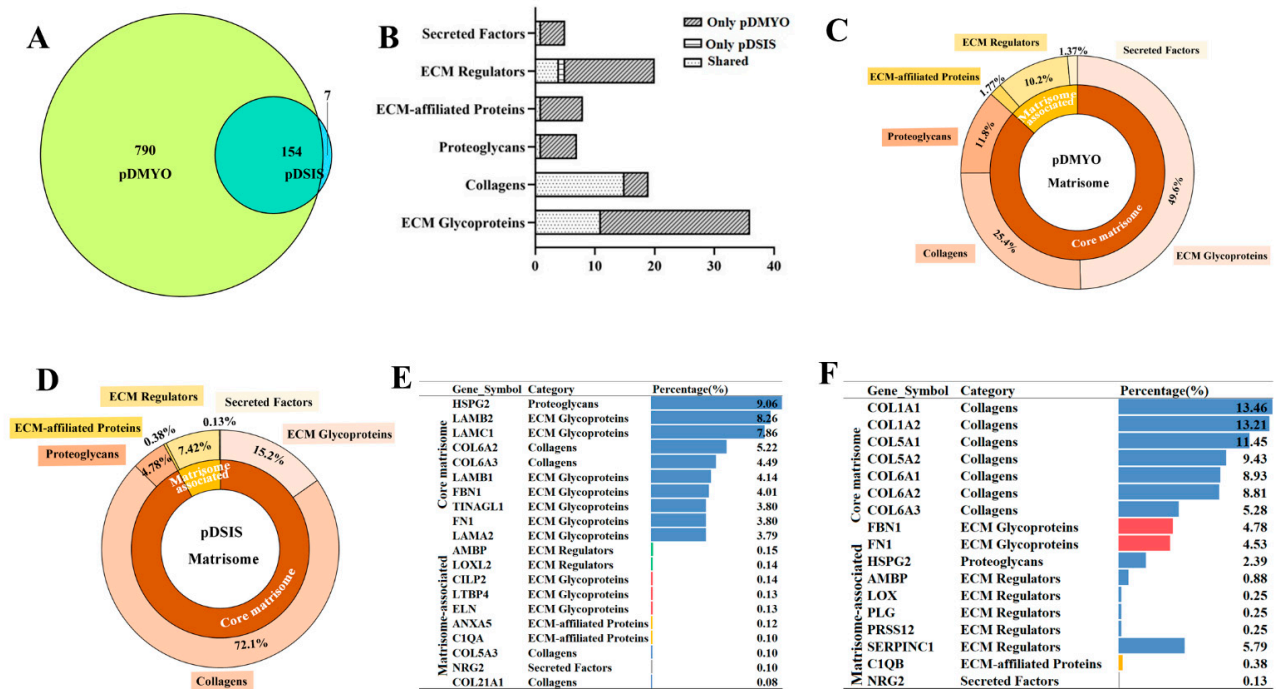


**Figure 4.** Proteomic analysis of pDMYO- and pDSIS-gels (A) Venn diagram of total proteins in pDMYO- and pDSIS-gels. (B) The common and unique matrisome proteins in pDMYO- and pDSIS-gels. (C) Types and proportion of matrisome proteins in pDMYO-gel. (D) Types and proportion of matrisome proteins in pDSIS-gel. (E) Top 10 matrisome proteins in pDMYO-gel. (F) Top 10 matrisome proteins in pDSIS-gel.

In addition, the top 10 proteins in pDMYO-gel were the glycoprotein HSPG2, laminins (LAMB2, LAMC1, LAMB1, FBN1, LAMA2), fibronectin (FN1), and collagen 6 (COL6A2, COL6A3) whereas the top ten proteins in pDSIS-gels were mostly collagen proteins, including COL6A3, COL1A1, COL6A2, COL6A1, COL1A2, FBN1, SERPINC1, COL5A2, HSPG2, and COL5A1 (Figure 4E,F). The relative gene expressions of matrisome proteins were shown in Figures S1 and S2. These results were consistent with the results in Figure 1, showing a higher collagen content in pDSIS than in pDMYO, whereas pDMYO contained more proteins of diverse molecular weights.

Figure S3 showed the relative abundance of proteins in pDMYO and pDSIS. Most common proteins expressed highly in both pDMYO and pDSIS belonged to collagen family, ECM glycoproteins, and proteoglycans, including COL1A2, COL6A2, COL1A1, COL4A2, COL6A1, DPT, FN1, and HSPG2. It has been reported that skin bridging protein (DPT) [22], fibronectin (FN1) [23], and heparan sulfate proteoglycan 2 (HSPG2) [24] can promote cell migration, adhesion, proliferation, and tissue repair. Therefore, we proposed that the presence of these proteins may participate in facilitating survival and viability of cardiomyocytes and endothelial cells.

There are only a few studies on proteomic analysis of decellularized myocardial matrix, especially for that derived from porcine. Dequach et al. [25] identified at least 14 kinds of protein components in porcine decellularized myocardial matrix. Diaz et al. [26] detected 28 distinct peptides in porcine decellularized myocardial matrix, which uniquely represent ECM and ECM-associated proteins. Johnson et al. [27] identified more than 200 proteins in the human decellularized myocardial matrix and also found unique proteins including agrin and alectin-1. Puig et al. [28] found 387 proteins in decellularized ventricle samples of zebrafish hearts and Cathepsin D was found in them. In our study, we found pDMYO contained 944 proteins. More importantly, we found some unique proteins in pDMYO, including annexin-6 (ANXA6) [29], agrin (AGRN) [30], cathepsin D (CTSD) [31] and galectin-1 (LGALS1) [32]. Studies have shown that ANXA6 physically interacts with sarcomeric  $\alpha$ -actinin and alters cardiomyocyte contractility, suggesting that ANXA6 may play an important role for the excitation and contraction of the cardiomyocytes [29]. Agrin has been proved to be able to promote cardiac regeneration in adult mice after myocardial infarction [30]. Myocardial CTSD upregulation induced by myocardial infarction protects against cardiac remodeling and malfunction [31]. Galectin-1 has emerged as key modulator of inflammatory processes, and recombinant Galectin-1 administration emerges as the most attractive approach for treatment of cardiovascular diseases, particularly acute myocardial infarction [32]. Galectin-1 in the pDMYO-gel may regulate the inflammatory response after myocardial infarction, and promote the repair of injured heart. This may explain the reason why cardiomyocytes can adhere, grow, spread, and maintain normal beating on pDMYO-gel. The proteomic analysis approach used in this study can be utilized as a means for comparing between complex natural biomaterials derived from different tissue sources or species, provides insight into protein composition of different ECM, and advances the field progress.

### 3.5. Effects of pDMYO- and pDSIS-Gels on Acute Myocardial Infarction in Rats

As shown in Figure 5A,B, LVEF and LVFS in pDSIS-gel, pDMYO-gel and PBS groups were significantly decreased, suggesting that the cardiac function of rats was significantly deteriorated due to myocardial infarction. The values of LVEF and LVFS in hydrogel groups were higher than those in PBS group, but the results were nonsignificant, indicating that the material may have a positive effect on improving the rat heart function. H&E staining (Figure 5C) showed that, compared with the sham group, the left ventricular cavity in PBS group was significantly enlarged and there was local collapse. The structure of the ventricular wall in the myocardial infarction area in PBS group was destroyed, and the ventricular wall became thinner, with a minimum thickness of 0.5 mm. The left ventricular cavity was smaller and the ventricular wall were thicker in pDSIS-gel and pDMYO-gel groups than that in PBS group. In pDMYO-gel group, the wall thickness was 1.3 mm. The

local magnified H&E-stained images (Figure 5D) showed that the myocardial matrix in the infarct border area of pDMYO-gel and pDSIS-gel groups was more uniform and denser than that of PBS group, and there were more microvessels in the infarct border area of pDMYO-gel and pDSIS-gel groups. Masson staining images (Figure 5E) showed that a large amount of collagen fibers (blue colour) was deposited in the myocardial infarction area. The length of infarction area in the hydrogel group was shorter than that in the PBS group, and the fibrosis level in the pDMYO-gel group was the lowest. The local magnified Masson-stained images of the infarct border area (Figure 5F) showed that there were less collagen fibers (blue colour) in pDMYO-gel group than that in PBS and pDSIS-gel groups.

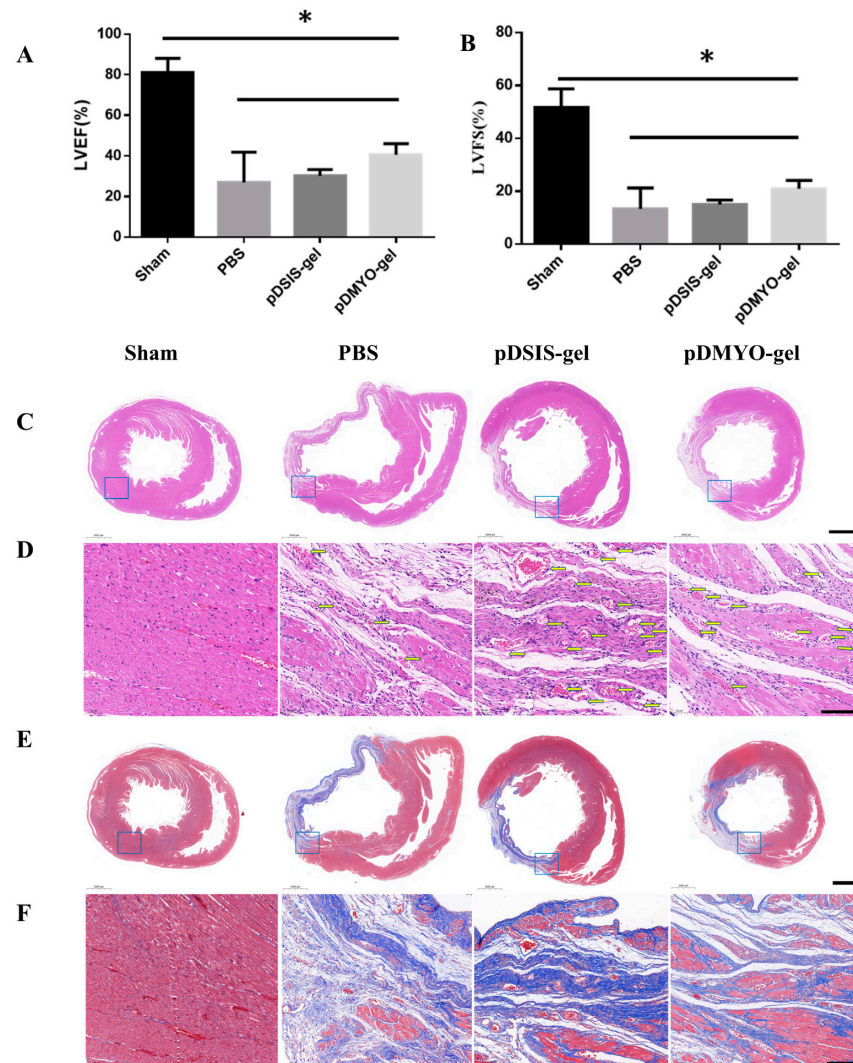


**Figure 5.** Effect of decellularized matrix hydrogels on acute myocardial infarction in rats (A) the effect of decellularized matrix hydrogels on left ventricular ejection fraction (LVEF). (B) the effect of decellularized matrix hydrogels on left ventricular shortening fraction (LVFS). (C) The H&E staining images of the rat heart sections (0.7 times magnification, the scale bar is 2000  $\mu\text{m}$ ); (D) The local magnified H&E-stained images of the infarct border area (18 times magnification, the magnified area is the blue box area in Figure 5C; the yellow arrow marks the location of the vessel; the scale bar is 100  $\mu\text{m}$ ); (E) the Masson staining images of the rat heart sections (0.7 times magnification, the scale bar is 2000  $\mu\text{m}$ ); (F) the local magnified Masson-stained images of the infarct border area (10 times magnification, the magnified area is the blue box area in Figure 5E). The collagen fibers were blue color, while the myocardial fibers were red color and the cell nuclei were blue black. The scale bar is 200  $\mu\text{m}$ ). \* denotes statistical difference within the same group with  $p < 0.05$ , respectively ( $n = 3$ ).

The above results indicate that pDMYO-gel has a better effect on improving cardiac function, inhibiting myocardial fibrosis, and maintaining ventricular wall thickness after acute myocardial infarction in rats, which is consistent with the results of cell culture study in vitro that pDMYO-gel is more conducive to maintaining myocardial cell viability.

#### 4. Conclusions

Although both pDMYO-gel, derived from cardiac tissues, and pDSIS-gel, derived from small intestinal submucosa, have a beneficial effect on the repair of myocardial injuries, they exert differential effects on the behavior of cardiomyocytes (NRCMs) and human umbilical vein endothelial cells (HUVECs), mainly due to their different protein components. pDSIS-gel is more conducive to the proliferation of HUVECs, while pDMYO-gel is more conducive to the adhesion, growth, spreading, and maintenance of the normal beating of NRCMs in vitro and pDMYO-gel has a better effect on improving cardiac function, inhibiting myocardial fibrosis, and maintaining ventricular wall thickness in acute myocardial infarction models in vivo. The unique proteins found in pDMYO, including annexin-6, agrin, cathepsin D, and galectin-1, may be the reason why pDMYO-gel has good performance in vitro and in vivo. The differential effects exerted by these two gels on cell has been correlated in this study. To design or prepare a close mimic of myocardial ECM for the repair of myocardial injuries, the molecular ingredients shall be considered to match with that of myocardial ECM, especially for some unique proteins. Further studies on the stoichiometric ratio of pDMYO-gel will help us understand how to design better materials for myocardial infarction repair and myocardial tissue engineering.

**Supplementary Materials:** The following are available online at <https://www.mdpi.com/article/10.3390/app11177768/s1>. Figure S1: Gene symbol and relative content of matrisome subgroup proteins of pDMYO matrix; Figure S2: Gene symbol and relative content of matrisome subgroup proteins of pDSIS matrix; Figure S3: the relative abundance of proteins in pDMYO and pDSIS; Video S1: the beating cardiomyocytes after seven days cultured on COL1-gel; Video S2: the beating cardiomyocytes after seven days cultured on pDSIS-gel; Video S3: the beating cardiomyocytes after seven days cultured on pDMYO-gel.

**Author Contributions:** Conceptualization and methodology, X.Y.; writing—original draft preparation, X.Y.; validation, S.C.; formal analysis, J.C.; resources, Y.L.; writing—review and editing, Y.B. and D.Q.; supervision, Y.B. and D.Q.; funding acquisition, S.Y. and D.Q. All authors have read and agreed to the published version of the manuscript.

**Funding:** This research was supported by Science and Technology Planning Project of Guangdong Province, China (2015B010125001).

**Institutional Review Board Statement:** All of the procedures involving animals in this study were approved by the Institutional Animal Care and Use Committee (IACUC), Sun Yat-Sen University (approval No. SYSU-IACUC-2020-000509). Animal welfare complied with the Laboratory Animal Guidelines for Ethical Review of Animal Welfare, General Administration of Quality Supervision, Inspection and Quarantine of the People's Republic of China/Standardization Administration of China (GB/T 35892-2018).

**Informed Consent Statement:** Not applicable.

**Data Availability Statement:** The data presented in this study are available in the article.

**Conflicts of Interest:** The authors declare no potential conflicts of interest.

#### References

1. Mukherjee, S.; Venugopal, J.R.; Ravichandran, R.; Ramakrishna, S.; Raghunath, M. Evaluation of the biocompatibility of PLACL/collagen nanostructured matrices with cardiomyocytes as a model for the regeneration of infarcted myocardium. *Adv. Funct. Mater.* **2011**, *21*, 2291–2300. [[CrossRef](#)]
2. Chang, M.Y.; Yang, Y.J.; Chang, C.H.; Tang, A.C.; Liao, W.Y.; Cheng, F.Y.; Yeh, C.S.; Lai, J.J.; Stayton, P.S.; Hsieh, P.C.H. Functionalized nanoparticles provide early cardioprotection after acute myocardial infarction. *J. Control. Release* **2013**, *170*, 287–294. [[CrossRef](#)] [[PubMed](#)]

3. Hashizume, R.; Fujimoto, K.L.; Hong, Y.; Guan, J.; Toma, C.; Tobita, K.; Wagner, W.R. Biodegradable elastic patch plasty ameliorates left ventricular adverse remodeling after ischemia-reperfusion injury: A preclinical study of a porous polyurethane material in a porcine model. *J. Thorac. Cardiovasc. Surg.* **2013**, *146*, 391–399.e1. [[CrossRef](#)] [[PubMed](#)]
4. Christman, K.L.; Fok, H.H.; Sievers, R.E.; Fang, Q.; Lee, R.J. Fibrin glue alone and skeletal myoblasts in a fibrin scaffold preserve cardiac function after myocardial infarction. *Tissue Eng.* **2004**, *10*, 403–409. [[CrossRef](#)] [[PubMed](#)]
5. Zimmermann, W.H.; Melnychenko, I.; Wasmeier, G.; Didié, M.; Naito, H.; Nixdorff, U.; Hess, A.; Budinsky, L.; Brune, K.; Michaelis, B. Engineered heart tissue grafts improve systolic and diastolic function in infarcted rat hearts. *Nat. Med.* **2006**, *12*, 452–458. [[CrossRef](#)]
6. Lu, W.; Lu, S.; Wang, H.; Li, D.; Duan, C.; Liu, Z.; Hao, T.; He, W.; Xu, B.; Fu, Q.; et al. Functional improvement of infarcted heart by co-injection of embryonic stem cells with temperature-responsive chitosan hydrogel. *Tissue Eng. Part A* **2009**, *15*, 1437–1447. [[CrossRef](#)]
7. Landa, N.; Miller, L.; Feinberg, M.S.; Holbova, R.; Leor, J. Effect of injectable alginate implant on cardiac remodeling and function after recent and old infarcts in rat. *Circulation* **2008**, *117*, 1388–1396. [[CrossRef](#)]
8. Ifkovits, J.L.; Tous, E.; Minakawa, M.; Morita, M.; Robb, J.D.; Koomalsingh, K.J.; Iii, J.H.G.; Gorman, R.C.; Langer, B.R. Injectable hydrogel properties influence infarct expansion and extent of post infarction left ventricular remodeling in an ovine model. *Proc. Natl. Acad. Sci. USA* **2010**, *107*, 11507–11512. [[CrossRef](#)]
9. Boyd, W.D.; Matheny, R.G.; Young, J.N.; Fallon, A.M. Injectable matrix bioscaffolds improve LV function and stimulate cardiomyocyte regeneration in infarcted hearts. *J. Heart Lung Transpl.* **2013**, *32*, S46. [[CrossRef](#)]
10. Francis, M.P.; Breathwaite, E.; Bulysheva, A.A.; Varghese, F.; Rodriguez, R.U.; Dutta, S.; Semenov, I.; Ogle, R.; Huber, A.; Tichy, A.M. Human placenta hydrogel reduces scarring in a rat model of cardiac ischemia and enhances cardiomyocyte and stem cell cultures. *Acta Biomater.* **2016**, *52*, 92–104. [[CrossRef](#)]
11. Singelyn, J.M.; Dequach, J.A.; Seif-Naraghi, S.B.; Littlefield, R.B.; Schup-Magoffin, P.J.; Christman, K.L. Naturally derived myocardial matrix as an injectable scaffold for cardiac tissue engineering. *Biomaterials* **2009**, *30*, 5409–5416. [[CrossRef](#)] [[PubMed](#)]
12. Saldin, L.T.; Cramer, M.C.; Velankar, S.S.; White, L.J.; Badylak, S.F. Extracellular matrix hydrogels from decellularized tissues: Structure and function. *Acta Biomater.* **2017**, *49*, 1–15. [[CrossRef](#)] [[PubMed](#)]
13. Roy, R.; Haase, T.; Nan, M.; Bader, A.; Stamm, C. Decellularized amniotic membrane attenuates postinfarct left ventricular remodeling. *J. Surg. Res.* **2016**, *200*, 409. [[CrossRef](#)] [[PubMed](#)]
14. Zou, J.; Liu, S.; Sun, J.; Yang, W.; Xu, Y.; Rao, Z.; Jiang, B.; Zhu, Q.; Liu, X.; Wu, J.; et al. Peripheral nerve-derived matrix hydrogel promotes remyelination and inhibits synapse formation. *Adv. Funct. Mater.* **2018**, *28*, 1705739. [[CrossRef](#)]
15. Xu, Y.; Zhou, J.; Liu, C.; Zhang, S.; Gao, F.; Guo, W.; Sun, X.; Zhang, C.; Li, H.; Rao, Z.; et al. Understanding the role of tissue-specific decellularized spinal cord matrix hydrogel for neural stem/progenitor cell microenvironment reconstruction and spinal cord injury. *Biomaterials* **2021**, *268*, 120596. [[CrossRef](#)]
16. Peng, Y.; Qing, X.; Lin, H.; Huang, D.; Li, J.; Tian, S.; Liu, S.; Lv, X.; Ma, K.; Li, R.; et al. Decellularized Disc Hydrogels for hBMSCs tissue-specific differentiation and tissue regeneration. *Bioact. Mater.* **2021**, *6*, 3541–3556. [[CrossRef](#)] [[PubMed](#)]
17. Ungerleider, J.L.; Johnson, T.D.; Hernandez, M.J.; Elhag, D.I.; Braden, R.L.; Dzieciatkowska, M.; Osborn, K.G.; Hansen, K.C.; Mahmud, E.; Christman, K.L. Extracellular Matrix Hydrogel Promotes Tissue Remodeling, Arteriogenesis, and Perfusion in a Rat Hindlimb Ischemia Model. *JACC Basic Transl. Sci.* **2016**, *1*, 32–44. [[CrossRef](#)]
18. Cunniffe, G.M.; Diaz-Payno, P.J.; Sheehy, E.J.; Critchley, S.E.; Almeida, H.V.; Pitacco, P.; Carroll, S.F.; Mahon, O.R.; Dunne, A.; Levingstone, T.J.; et al. Tissue-specific extracellular matrix scaffolds for the regeneration of spatially complex musculoskeletal tissues. *Biomaterials* **2019**, *188*, 63–73. [[CrossRef](#)]
19. Ji, Y.; Zhou, J.; Sun, T.; Tang, K.; Xiong, Z.; Ren, Z.; Yao, S.; Chen, K.; Yang, F.; Zhu, F. Diverse preparation methods for small intestinal submucosa (SIS): Decellularization, components, and structure. *J. Biomed. Mater. Res. A* **2019**, *107*, 689–697. [[CrossRef](#)]
20. Crapo, P.M.; Gilbert, T.W.; Badylak, S.F. An overview of tissue and whole organ decellularization processes. *Biomaterials* **2011**, *32*, 3233–3243. [[CrossRef](#)]
21. Wang, R.M.; Christman, K.L. Decellularized myocardial matrix hydrogels: In basic research and preclinical studies. *Adv. Drug Deliv. Rev.* **2016**, *96*, 77–82. [[CrossRef](#)]
22. Lewandowska, K.; Choi, H.U.; Rosenberg, L.C.; Sasse, J.; Culp, L.A. Extracellular matrix adhesion-promoting activities of a dermatan sulfate proteoglycan-associated protein (22K) from bovine fetal skin. *J. Cell Sci.* **1991**, *99*, 657–668. [[CrossRef](#)]
23. Hynes, R.O.; Yamada, K.M. Fibronectins: Multifunctional modular glycoproteins. *J. Cell Biol.* **1982**, *95*, 369–377. [[CrossRef](#)]
24. Allen, B.L.; Filla, M.S.; Rappaegeer, A.C. Role of heparan sulfate as a tissue-specific regulator of FGF-4 and FGF receptor recognition. *J. Cell Biol.* **2001**, *155*, 845–857. [[CrossRef](#)]
25. Dequach, J.A.; Mezzano, V.; Miglani, A.; Lange, S.; Christman, K.L. Simple and high yielding method for preparing tissue specific extracellular matrix coatings for cell culture. *PLoS ONE* **2010**, *5*, e13039. [[CrossRef](#)] [[PubMed](#)]
26. Diaz, M.D.; Tran, E.; Wassenaar, J.W.; Spang, M.; Christman, K.L. Injectable myocardial matrix hydrogel mitigates negative left ventricular remodeling in a chronic myocardial infarction model. *JACC Basic Transl. Sci.* **2021**, *6*, 350–361. [[CrossRef](#)] [[PubMed](#)]
27. Johnson, T.D.; Hill, R.C.; Dzieciatkowska, M.; Nigam, V.; Behfar, A.; Christman, K.L.; Hansen, K.C. Quantification of decellularized human myocardial matrix: A comparison of six patients. *Proteom. Clin. Appl.* **2016**, *10*, 75–83. [[CrossRef](#)]

28. Garcia-Puig, A.; Mosquera, J.L.; Jiménez-Delgado, S.; García-Pastor, C.; Jorba, I.; Navajas, D.; Canals, F.; Raya, A. Proteomics Analysis of Extracellular Matrix Remodeling During Zebrafish Heart Regeneration. *Mol. Cell Proteom.* **2019**, *18*, 1745–1755. [[CrossRef](#)]
29. Mishra, S.; Chander, V.; Banerjee, P.; Oh, J.G.; Bandyopadhyay, A. Interaction of annexin a6 with alpha actinin in cardiomyocytes. *BMC Cell Biol.* **2011**, *12*, 7. [[CrossRef](#)]
30. Bassat, E.; Mutlak, Y.E.; Genzelinakh, A.; Shadrin, I.Y.; Umansky, K.B.; Yifa, O.; Kain, D.; Rajchman, D.; Leach, J.; Bassat, D.R. The extracellular matrix protein agrin promotes heart regeneration in mice. *Nature* **2017**, *547*, 179–184. [[CrossRef](#)] [[PubMed](#)]
31. Wu, P.; Yuan, X.; Li, F.; Zhang, J.; Zhu, W.; Wei, M.; Li, J.; Wang, X. Myocardial upregulation of cathepsin d by ischemic heart disease promotes autophagic flux and protects against cardiac remodeling and heart failure. *Circ. Heart Fail.* **2017**, *10*, e004044. [[CrossRef](#)]
32. Seropian, I.M.; González, G.E.; Maller, S.M.; Berrocal, D.H.; Rabinovich, G.A. Galectin-1 as an emerging mediator of cardiovascular inflammation: Mechanisms and therapeutic opportunities. *Mediat. Inflamm.* **2018**, *2018*, 1–11. [[CrossRef](#)] [[PubMed](#)]